Molecular Therapy
Nucleic Acids
Original Article

# Synthetic mRNA delivered to human cells leads to expression of Cpl-1 bacteriophage-endolysin with activity against *Streptococcus pneumoniae*

Moritz K. Jansson,[1] Dat Tien Nguyen,[1] Stefan Mikkat,[2] Carolin Warnke,[1] Marc Benjamin Janssen,[1] Philipp Warnke,[1] Bernd Kreikemeyer,[1,3] and Nadja Patenge[1,3]

[1]Institute of Medical Microbiology, Virology and Hygiene, University Medicine Rostock, Rostock, Germany; [2]Core Facility Proteome Analysis, University Medicine Rostock, Rostock, Germany

**Endolysins are bacteriophage-encoded hydrolases that show high antibacterial activity and a narrow substrate spectrum. We hypothesize that an mRNA-based approach to endolysin therapy can overcome some challenges of conventional endolysin therapy, namely organ targeting and bioavailability. We show that synthetic mRNA applied to three human cell lines (HEK293T, A549, HepG2 cells) leads to expression and cytosolic accumulation of the Cpl-1 endolysin with activity against *Streptococcus pneumoniae*. Addition of a human lysozyme signal peptide sequence translocates the Cpl-1 to the endoplasmic reticulum leading to secretion (hlySP-sCpl-1). The pneumococcal killing effect of hlySP-sCpl-1 was enhanced by introduction of a point mutation to avoid N-linked-glycosylation. hlySP-sCpl-1N215D, collected from the culture supernatant of A549 cells 6 h post-transfection showed a significant killing effect and was active against nine pneumococcal strains. mRNA-based cytosolic Cpl-1 and secretory hlySP-sCpl-1N215D show potential for innovative treatment strategies against pneumococcal disease and, to our best knowledge, represent the first approach to mRNA-based endolysin therapy. We assume that many other bacterial pathogens could be targeted with this novel approach.**

## INTRODUCTION

Bacteriophage-encoded proteins such as endolysins could offer a solution to the antibiotic resistance crisis. Endolysins are peptidoglycan hydrolases translated at the end of the bacteriophage lytic cycle that destruct the bacterial cell wall inside their host organisms in an act termed "lysis from within." Gram-positives can readily be lysed "from without" due to their exposed peptidoglycan layer.[1] Encouragingly, no resistance mechanisms or bacteria losing sensitivity to endolysins have been reported.[2]

Over recent years, research on endoylsins has led to an improved understanding of their applicability to treat specific forms of bacterial diseases such as endocarditis or pneumonia and human trials are ongoing.[3] Despite recent improvements to almost all aspects of endolysin therapy, organ-specific targeting and bioavailability are among the remaining challenges in the current approach of exogenous administration of recombinantly produced endolysins to an infected organism.[1] Given their proteinaceous nature, transporting endolysins to the site of infection is not straightforward due to numerous barriers in the human body. For most endolysins, targeting intracellular compartments is only feasible after modifications such as fusion to cell-penetrating peptides.[3] Intravenous applications are often limited by short serum half-life ranging from minutes to several hours due to tissue distribution, degradation by proteases, inactivation by antibodies, and renal excretion.[4,5]

Since the discovery of mRNA molecules in the 1960s, a deeper understanding of their functioning has led to an ongoing revolution in medical fields ranging from vaccinology to cancer research.[6] While several mRNA-based antiviral therapies are under investigation,[7–13] the concept of mRNA-based antibacterial therapies seems to be comparatively underexplored. In a pioneering study dating more than 20 years ago, Kisich et al. demonstrated that human β-defensin mRNA, which is normally not expressed in alveolar macrophages, was capable of restricting intracellular growth of *Mycobacterium tuberculosis*.[14] More recently, Hou et al. used adoptive transfer of macrophages that had been transfected *ex vivo* with mRNA encoding antimicrobial peptide IB367 to treat sepsis caused by multiple drug-resistant strains of *E. coli* and *Staphylcoccus aureus* in mice with immunosuppression.[15] To the best of the authors' knowledge, mRNA-based endolysin therapies have not been described. With respect to endolysin therapy, an mRNA-based therapy approach encompasses the administration of endolysin-encoding mRNA molecules to enable the recipient organism to endogenously produce the endolysin in question.

mRNA delivery vehicles can specifically reach organs such as the liver, vascular endothelium, the spleen, or the lungs.[6,16–23] Notably, the

Received 20 July 2023; accepted 6 February 2024;
https://doi.org/10.1016/j.omtn.2024.102145.

[3]These authors contributed equally

**Correspondence:** Moritz K. Jansson, Institute of Medical Microbiology, Virology and Hygiene, University Medicine Rostock, Rostock, Germany.
**E-mail:** moritz.jansson@med.uni-rostock.de

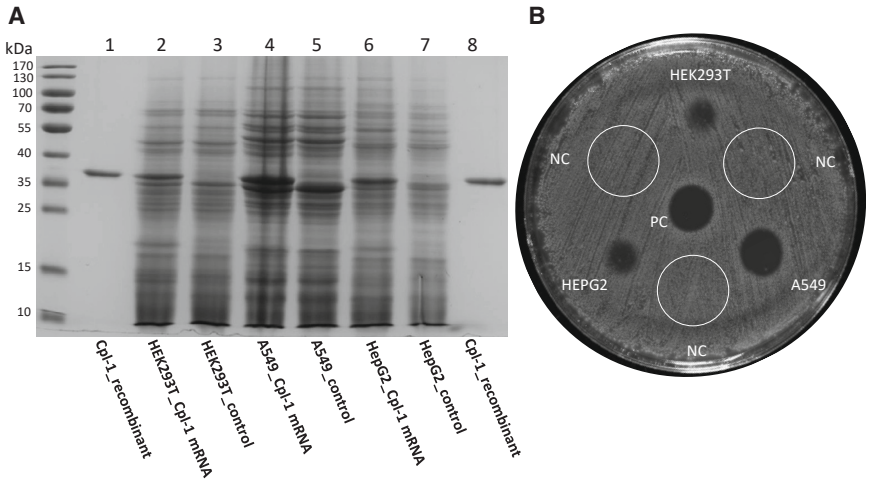


**Figure 1. Investigation of lysates of cells transfected with Cpl-1-encoding mRNA**

(A) cell lysates of HEK293T (2) A549 (4) and HepG2 (6) cells harvested 24 h after transfection with Cpl-1-encoding mRNA were subjected to SDS-PAGE. Each sample is followed by a control (3, 5, 7); 1 and 8: recombinant Cpl-1 (1.75 μg, ca. 37 kDa). (B) Assessment of lysis zones on blood agar plate. The plate was inoculated with pneumococcal suspension (Mc Farland 0.5). Ten microliters of lysate from HEK293T, A549, HepG2 cells harvested 24 h after transfection with Cpl-1-encoding mRNA was spotted on plate 16 h before readout. NC, negative controls were applied within area of the white circle; PC, 10 μL of recombinant Cpl-1 (10 μg/mL) was dropped in center of each plate as positive control.

mRNA platform is highly adaptable and could be used for delivery of mRNA constructs encoding suitable endolysins independent of their proteinaceous characteristics.[24]

Following cytosolic delivery of *in vitro*-transcribed (IVT) mRNA, translation and thus protein production begins and continues for a time frame that depends on the stability of the mRNA. Elements adding to cytosolic stability of mRNA comprise modifications of the 5′ cap, 5′ and 3′ untranslated regions (UTRs), 3′ poly(A) tail, and nucleotide substitutions such as replacing uridine with N1-methylpseudouridine (m1ψ).[6,25] Depending on the choice of these elements, protein translation can last hours to days.[26,27] Therefore, an mRNA-based approach to endolysin therapy might reduce or even eliminate the need of repetitive dosing. Furthermore, translation and consecutive protein production inside cells might facilitate intracellular targeting of pathogens. Finally, there are other more general advantages of mRNA therapies comprising rapid and cost-effective production compared with their protein-based equivalents and adaptability to evolving pathogens.[24]

The aim of the present study was to investigate the feasibility of an mRNA-based approach to endolysin production in human cells. To this end, the Cpl-1 endolysin, a 37-kDa lysozyme derived from Cp-1, a small virulent bacteriophage infecting *Streptococcus pneumoniae,* was chosen as a model endolysin.[28] Following the first description of Cpl-1 in 1987, its various properties as a therapeutic agent against pneumococcal disease have been extensively investigated both on a molecular and animal infection model basis. For instance, it showed promising results when used for treatment of pneumococcal carriage, non-invasive and invasive disease.[5,28–32] *S. pneumoniae,* a gram-positive encapsulated pathogen, is a leading cause of upper and lower respiratory disease such as sinusitis, otitis media, and pneumonia. It is estimated that *S. pneumoniae* caused 829,000 (682,000–1,010,000) deaths among all age groups in 2019 and was the pathogen associated with the most deaths among children younger than 5 years.[33] Due to considerable antibiotic resistance in some regions,[34] *S. pneumoniae* has been placed on the World Health Organization 2017 list of bacteria for which new antibiotics are urgently needed.[35]

## RESULTS

### Cpl-1-encoding mRNA was translated into Cpl-1 endolysin in human cell lines

mRNA constructs were stabilized using the 5′ and 3′ UTR regions of the human alpha globin gene, a cap-1 structure and a poly(A) tail of 120 bases was used as previously described.[25,26] Uridine was completely substituted with N1-methylpseudouridine to improve translation efficiency and reduce mRNA immunogenicity.[36] HEK293T cells were used as they represent a human cell line that can be easily transfected. As the pneumococcus is a common cause of lower respiratory disease A549 cells were used as a model of alveolar epithelium of the human lung.[33] HepG2 cells were used to model hepatocytes. Since the liver is a metabolically active organ that can be efficiently transfected, it could be employed for the synthesis and systemic secretion of mRNA-based endolysins.[22] HEK293T, A549, and HepG2 cells, respectively, were transfected with Cpl-1-encoding mRNA. The nucleotide sequence of the Cpl-1-encoding mRNA is presented in Table S1. Twenty-four hours post-transfection, cells were lysed and lysates of Cpl-1 mRNA-transfected and non-transfected cells were subjected to SDS-PAGE. A distinct band with a comparable molecular weight to recombinantly expressed Cpl-1 was observed exclusively in lysate samples of mRNA-transfected cells (Figure 1A). Similarly, western blot analysis of the lysate samples from Cpl-1 mRNA-transfected cells showed prominent bands with a comparable molecular weight to recombinantly expressed Cpl-1 and some less prominent bands with lower molecular weight. As these bands were only present in Cpl-1 mRNA-transfected cells and targeted by the polyclonal Cpl-1 antibody, the bands were considered to represent the Cpl-1 endolysin and its degradation products (Figure S1). Lysates were applied to blood agar plates inoculated with *S. pneumoniae* suspension (McFarland Standard of 0.5). Cell lysates from all three cell lines caused a lysis zone, whereas no lysis zone was observed from cell lysates derived from non-transfected controls (Figure 1B).

Twenty-two microliters of the respective lysates was added to 200 μL of pneumococcal suspension. $OD_{600}$ was measured for 60 min, followed by determination of the bacterial counts (Figure 2). Bacterial suspensions treated with lysates from mRNA-transfected cells showed a pronounced $OD_{600}$ reduction over time (Figures 2A, 2C, and 2E). After 60 min, the colony counts of bacterial suspensions treated with lysates of mRNA-transfected cells were significantly lower when compared with samples treated with control lysates, showing a log reduction of 1.89 for HEK293T ($p < 0.001$, $t = 4.87$, $df = 12$), 2.72 for A549 ($p < 0.01$, $t = 4.04$, $df = 13$), and 1.62 for HepG2 ($p < 0.01$, $t = 3.91$, $df = 8$) cells (Figures 2B, 2D, and 2F). In contrast, pneumococcal suspensions treated with supernatants of Cpl-1 mRNA-transfected cells showed a less pronounced reduction of $OD_{600}$ and colony counts compared with samples treated with cell lysates. The respective log reduction in comparison with samples treated with supernatants of non-transfected control cells was 0.41 for HEK293T ($p = 0.16$, $t = 1.54$, $df = 8$), 0.07 for A549 ($p = 0.76$, $t = 0.32$, $df = 11$), and 0.53 for HepG2 ($p = 0.08$, $t = 1.94$, $df = 9$) cells. To exclude the possibility of an unspecific pneumococcal killing effect as a response to externally added Cpl-1 mRNA to the cell lines, transfection experiments were repeated using Cypridina Luciferase-encoding mRNA instead of Cpl-1 encoding mRNA. No killing effect could be observed from lysate or supernatant samples in turbidity reduction experiments. The results of these negative control experiments are shown in Figure S2.

Three independent lysate samples of Cpl-1 mRNA-transfected cells from each cell line were subjected to mass spectrometry. Cpl-1 was the most abundant protein in cell lines HEK293T and A549 and the second most abundant protein after glyceraldehyde-3-phosphate dehydrogenase in HepG2 cells. On average, the Cpl-1 endolysin accounted for 2.5%, 4.5%, and 1.9% of the total protein mass in HEK293T, A549, and HepG2 cells, respectively. Peptide mapping analysis revealed N-terminal methionine excision and the complete C terminus of Cpl-1. The lack of coverage of some internal sequence regions can be largely explained by unfavorable arrangement of trypsin cleavage sites (Figure S3). Immunocytochemistry analysis (ICC) of A549 cells using a polyclonal Cpl-1 primary antibody was performed to characterize the localization of the Cpl-1 endolysin. The staining pattern suggested cytosolic presence of Cpl-1 (Figure 3).

The results suggest that the Cpl-1 endolysin-encoding mRNA was translated in all three human cells lines, resulting in a biologically active form of Cpl-1 primarily residing within the cytosol.

### Signal peptides led to secretion of the Cpl-1 endolysin into the culture medium

Most secretory proteins are equipped with a short N-terminal amino acid sequence called signal peptide (SP). SPs target nascent proteins to the secretory pathway via the endoplasmic reticulum in eukaryotes and facilitate translocation across the plasma membrane in prokaryotes.[37] Although SP sequences are highly diverse both in length and in amino acid composition, they share a conserved structure. In numerous studies, native SPs have been replaced with the aim of optimizing secretion levels in mammalian expression systems.[38–41] SPs previously used for heterologous expression of secretory proteins were employed to convert the Cpl-1 endolysin into a secretory protein (from here on denoted as sCpl-1). mRNA constructs were created that included one of the following seven SPs between the start codon and the 5′ end of the Cpl-1 endolysin open reading frame: an artificially created SP termed secrecon[42] (secSP-sCpl-1) and its variant with two additional alanine residues[38] (secAASP-sCpl-1), and SPs derived from human serum albumin (halSP-sCpl-1), azurocidin (hazSP-sCpl-1), lysozyme (hlySP-sCpl-1), immunoglobulin heavy chain (hIgHCSP-sCpl-1),[39] and the SARS-CoV-2 spike protein (SARSspSP-sCpl-1) (Table S2). To screen for activity, turbidity reduction experiments were conducted as described using concentrated supernatants collected 24 h post-transfection. Supernatants collected from all samples transfected with any of the seven mRNA constructs caused reduction of turbidity. The extent of reduction was dependent on the SP fused to the Cpl-1 sequence (Figure S4). In all supernatant samples of sCpl-1 mRNA-transfected cells subjected to SDS-PAGE, a distinct band could be detected migrating more slowly than the recombinantly expressed Cpl-1, indicating an increased molecular weight of the sCpl-1 endolysin (Figures 4A–4C). Slightly below, a less prominent band with comparable size to recombinant Cpl-1 was visible in supernatants from HEK293T and A549 cells but absent in supernatants from HEPG2 cells. Other protein bands visible on the gels were present both in supernatants of mRNA-transfected cells as well as the non-transfected controls and were considered to represent physiologically secreted proteins.

Based on the results of turbidity reduction experiments and SDS-PAGE, the sCpl-1-encoding mRNA construct employing the human lysozyme SP was chosen for further analysis (hlySP-sCpl-1).

Mass spectrometric peptide mapping of secreted hlySP-sCpl-1 revealed N-terminal amino acid coverage starting at the putative cleavage site of the human lysozyme SP (Figure S3B). Therefore, it was considered unlikely that the mass increase observed in SDS-PAGE had been caused by an uncleaved SP.

### The hlySP-sCpl-1 endolysin was modified by N-linked glycosylation

Post-translational modifications (PTMs) in the secretory pathway of eukaryotic cells were considered as a possible explanation for the increased molecular weight of sCpl-1. A PTM common to secretory proteins in eukaryotic cells is the addition of oligosaccharides to the nitrogen atom of an asparagine residue in a process termed N-linked glycosylation.[43] Attachment of oligosaccharides to the asparagine residue is mediated by the consensus sequence Asn–X–Ser/Thr, where X is permitted to be any amino acid except proline.[44] As the amino acid sequence of the Cpl-1 endolysin contains a recognition site for N-linked glycan attachment in amino acid positions 215–217 (Asn-Gly-Ser), glycosylation of the sCpl-1 was investigated. In a first step, PNGase F, an enzyme capable of removing N-linked glycans, was applied to hlySP-sCpl-1-containing concentrated

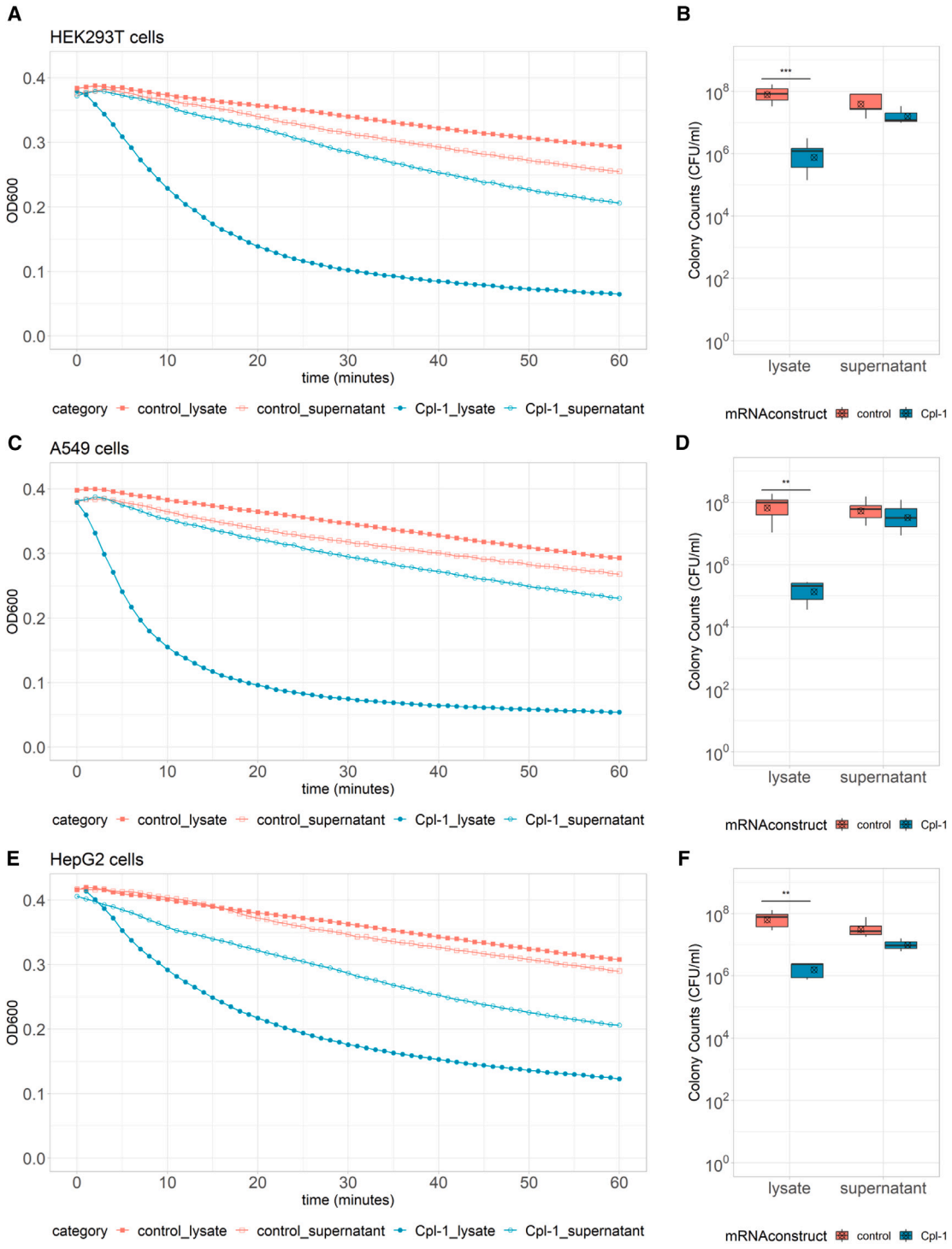


**Figure 2. Bacteriolytic effect of lysates and concentrated supernatant samples from HEK293T/A549/HepG2 cells transfected with Cpl-1-encoding mRNA against *S. pneumoniae***

(A, C, E) Turbidity reduction experiments. Twenty-two microliters of lysate, concentrated supernatant, or control samples was applied to 200 μL of pneumococcal suspension in PBS (pH 7.0). Data from representative experiments are shown. (B, D, F) After turbidity measurements, samples were plated on blood agar and CFUs were counted after 16 h. Data are based on at least three independent experiments. Boxplots represent minimum, maximum, and median values, and the interquartile range. The mean is represented by a crossed circle, p values <0.05 are indicated (*p < 0.05–0.01; **p < 0.01–0.001; ***p < 0.001).

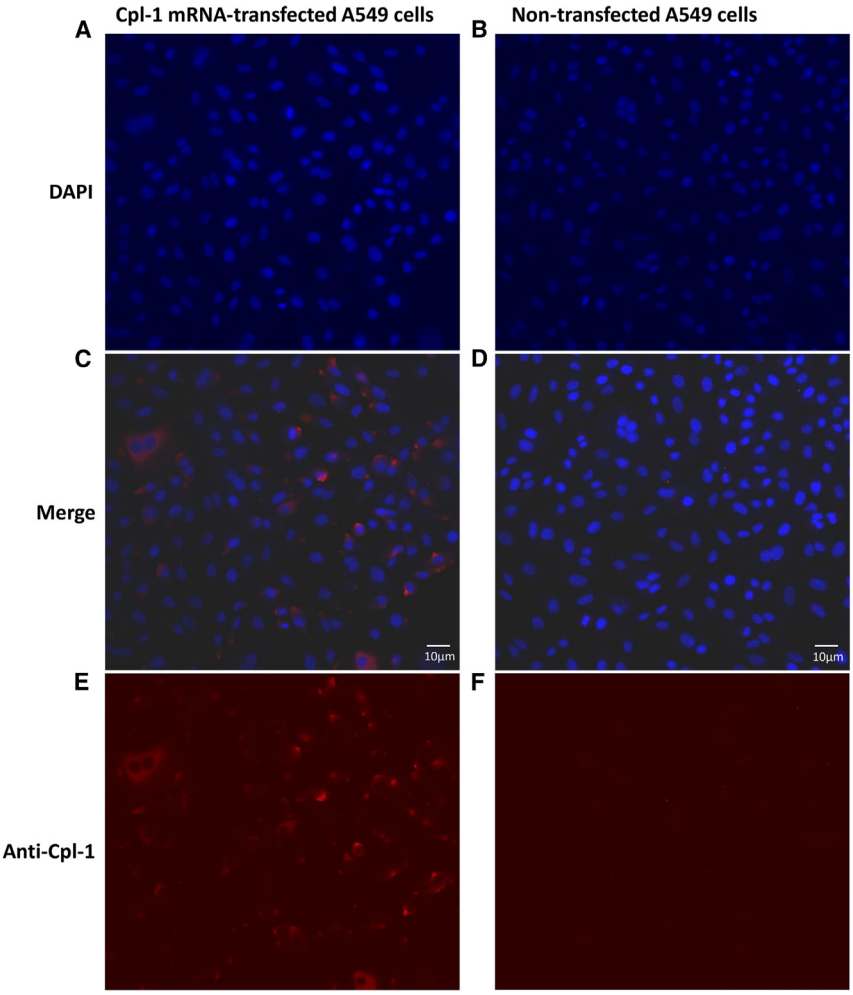


**Figure 3. Immunofluorescent staining of Cpl-1 mRNA-transfected A549 cells**

The cells were stained using an anti-Cpl-1 rabbit-derived antibody and conjugated goat anti-rabbit secondary antibody, DAPI was used for staining of cell nuclei. The panels show DAPI (A and B), DAPI + Anti-Cpl-1 (C and D), and Anti-Cpl-1 (E and F) -stained cells of Cpl-1 mRNA-transfected and non-transfected cells, respectively. Pictures were taken at ×200 magnification.

supernatants from all three cell lines under denaturing conditions. Following PNGase F treatment, the hlySP-sCpl-1 band showed comparable molecular weight to recombinant Cpl-1 in SDS-PAGE (Figure 4D). To further investigate the effect of PNGase F treatment on enzymatic activity of hlySP-sCpl-1, PNGase F digestion was conducted under non-denaturing conditions and equal volumes of PNGase F-treated and -untreated samples were subjected to turbidity reduction assays. After PNGase F treatment, hlySP-sCpl-1 showed an increased pneumococcal killing effect compared with PNGase F non-treated hlySP-sCpl-1 ($p = 0.06$, $t = 2.60$, $df = 4$) (Figure S5).

### N-linked glycosylation of the hlySP-sCpl-1 endolysin could be prevented by removal of the glycosylation site and was found to affect biological activity

Next, the amino acid sequence of hlySP-sCpl-1 was modified by introduction of point mutations at the consensus sequence for N-linked glycosylation. Two mRNA constructs were synthesized, the first comprising the mutation r.694A>G to code for aspartate in position 215 instead of asparagine (hlySP-sCpl-1N215D), the second comprising the mutations r.700A>G and r.701G>C to code for alanine in position 217 instead of serine (hlySP-sCpl-1S217A) (amino acid positions are indicated as for the Cpl-1 wild-type sequence, not accounting for the 17 additional amino acids of the human lysozyme SP of hlySP-sCpl-1). Both amino acid exchanges resulted in hlySP-sCpl-1 proteins whose molecular weight matched the recombinant Cpl-1 endolysin, indicating that no glycosylation occurred when the mutant proteins were expressed in human cells (Figure 5A).

Screening of concentrated supernatants of cells that had been transfected with hlySP-sCpl-1/hlySP-sCpl-1N215D/hlySP-sCpl-1S217A-encoding mRNA by assessment of pneumococcal lysis zones on blood agar plates showed pneumococcal clearing in a construct-dependent fashion (Figures 5B–5D). hlySP-sCpl-1 and hlySP-sCpl-1S217A derived from HEK293T and HepG2 supernatants caused no or incomplete bacterial clearing, while both variants collected from A549 cells caused a clear lysis zone (Figure 5C).

Concentrated supernatant from all three cell lines resulted in a prominent clearing zone after hlySP-sCpl-1N215D-encoding mRNA transfection. Turbidity reduction assays conducted with consecutive determination of colony-forming unit (CFU) reduction confirmed a more pronounced pneumococcal killing effect of samples containing hlySP-sCpl-1N215D compared with hlySP-sCpl-1 and hlySP-sCpl-1S217A. The effect was more evident in supernatants from HEK293T (log reductions: 2.58 [$p < 0.01$] vs. 1.92 [$p = 0.01$] and 1.76 [$p = 0.01$], respectively) and HepG2 cells (log reductions: 2.25 [$p < 0.001$] vs. 1.54 [$p < 0.01$] and 1.36 [$p < 0.01$], respectively) than from A549 cells (log reductions: 2.63 [$p < 0.001$] vs. 2.37 [$p < 0.001$] and 2.32 [$p < 0.001$], respectively) (Figure 6). The hlySP-sCpl-1N215D mutant was therefore used in all further analysis. The nucleotide sequence of the hlySP-sCpl-1N215D-encoding mRNA is presented in Table S1.

Three biologically independent samples of hlySP-sCpl-1N215D mRNA-transfected cells from each cell line were subjected to mass

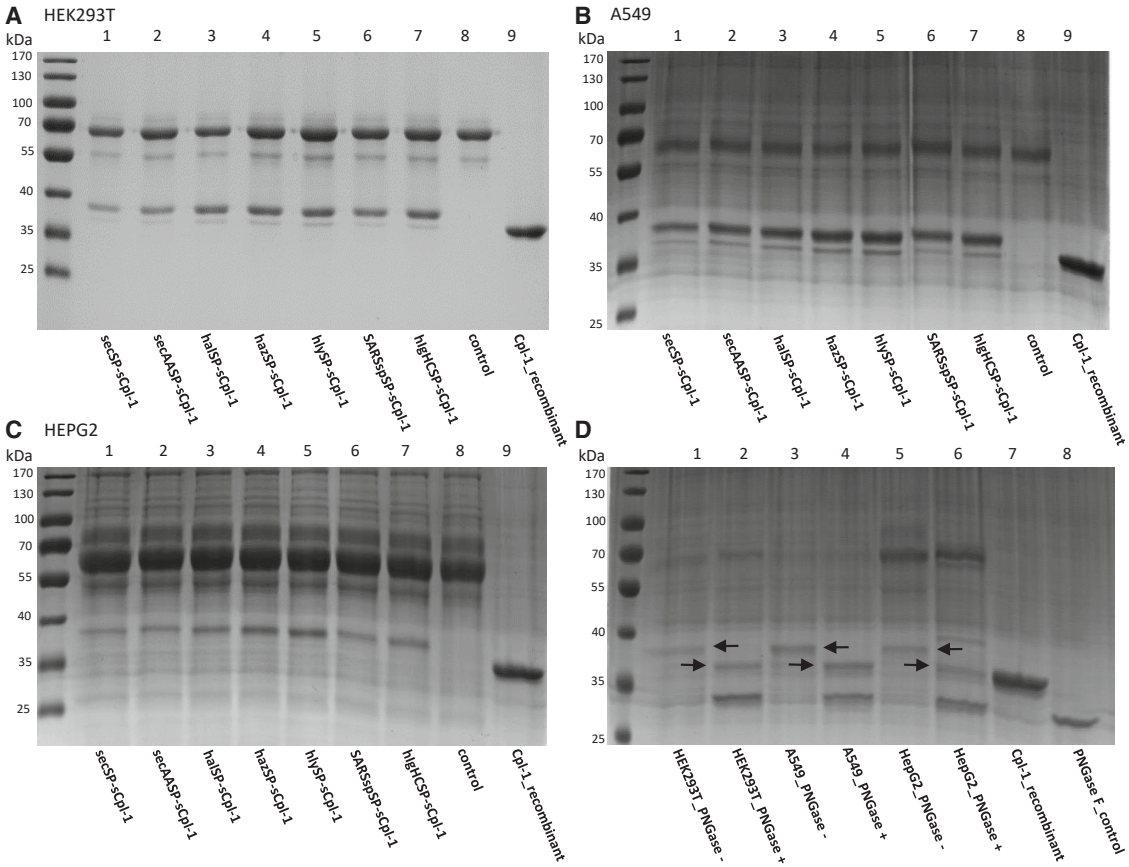


**Figure 4. SDS-PAGE of concentrated serum-free culture supernatant samples of cells transfected with sCpl-1 encoding mRNA**

HEK293T (A), A549 (B), and HepG2 (C) cells were transfected with mRNA encoding sCpl-1 and different signal peptides as designated in the corresponding lane. The prominent band of the sCpl-1 protein running a few kDa above the 37-kDa band of recombinant Cpl-1 in samples from HEK293T and A549 cells is considered to be caused by glycosylation of the majority of sCpl-1 (A and B), while all of sCpl-1 seems to be glycosylated in samples from HEPG-2 cells (C). (D) HEK293T, A549, and HepG2 cells were transfected with mRNA encoding hlySP-sCpl-1 and treated with PNGase F. Lanes 1 and 2 represent supernatant containing hlySP-sCpl-1 derived from HEK293T cells, 3 and 4 from A549 cells, 5 and 6 from HepG2 cells before and after PNGase F digestion (labeled either PNGase− or PNGase+, respectively); (→: rightwards arrows mark PNGase F digested Cpl-1 bands; ←: leftwards arrows mark PNGase F undigested Cpl-1 bands; recombinant Cpl-1 (7) (1.75 μg, ca. 37 kDa).

spectrometry. Figure S3B shows the amino acid coverage of the hlySP-sCpl-1N215D sequence. On average, the hlySP-sCpl-1N215D endolysin represented 46.8%, 47.6%, and 8.1% of human protein identified in the supernatant of HEK293T, A549, and HepG2 cells, respectively (Table S3). To estimate the hlySP-sCpl-1N215D concentration in supernatants, total protein concentrations in the samples were quantified using the Qubit protein assay and multiplied with the respective percentage of hlySP-sCpl-1N215D (Table S3). The concentration of hlySP-sCpl-1N215D in unconcentrated supernatants (equal to the final concentration in turbidity reduction assays) was estimated to be 3.9 μg/mL for HEK293T, 3.6 μg/mL for A549, and 3.0 μg/mL for HepG2 cells.

### There was no evidence of self-killing of *S. pneumoniae* by hlySP-sCpl-1N215D-encoding mRNA

The possibility of residual IVT-mRNA potentially present in the samples leading to translation by *S. pneumoniae* and consecutive self-destruction was taken into consideration. To test this hypothesis, turbidity reduction experiments were conducted with 500 ng of hlySP-sCpl-1N215D-encoding mRNA prepared with Lipofectamine MessengerMAX (Thermo Fisher Scientific) in 50 μL Opti-MEM reduced serum medium (Thermo Fisher Scientific) as described for transfection of cell lines. Relative to controls, no reduction in turbidity was observed (Figure S6) and there was no significant difference between log mean colony counts (0.09, $p = 0.63$, $t = -0.51$, $df = 4$).

### mRNA dose affected hlySP-sCpl-1N215D expression in a cell-dependent fashion

Transfection experiments were repeated for all three cell lines using different doses of hlySP-sCpl-1N215D-encoding mRNA (250 ng, 500 ng, 1,000 ng). Culture supernatant was collected 24 h after transfection and processed as described. Turbidity reduction experiments (Figures S7A–S7C) and subsequent determination of CFU were

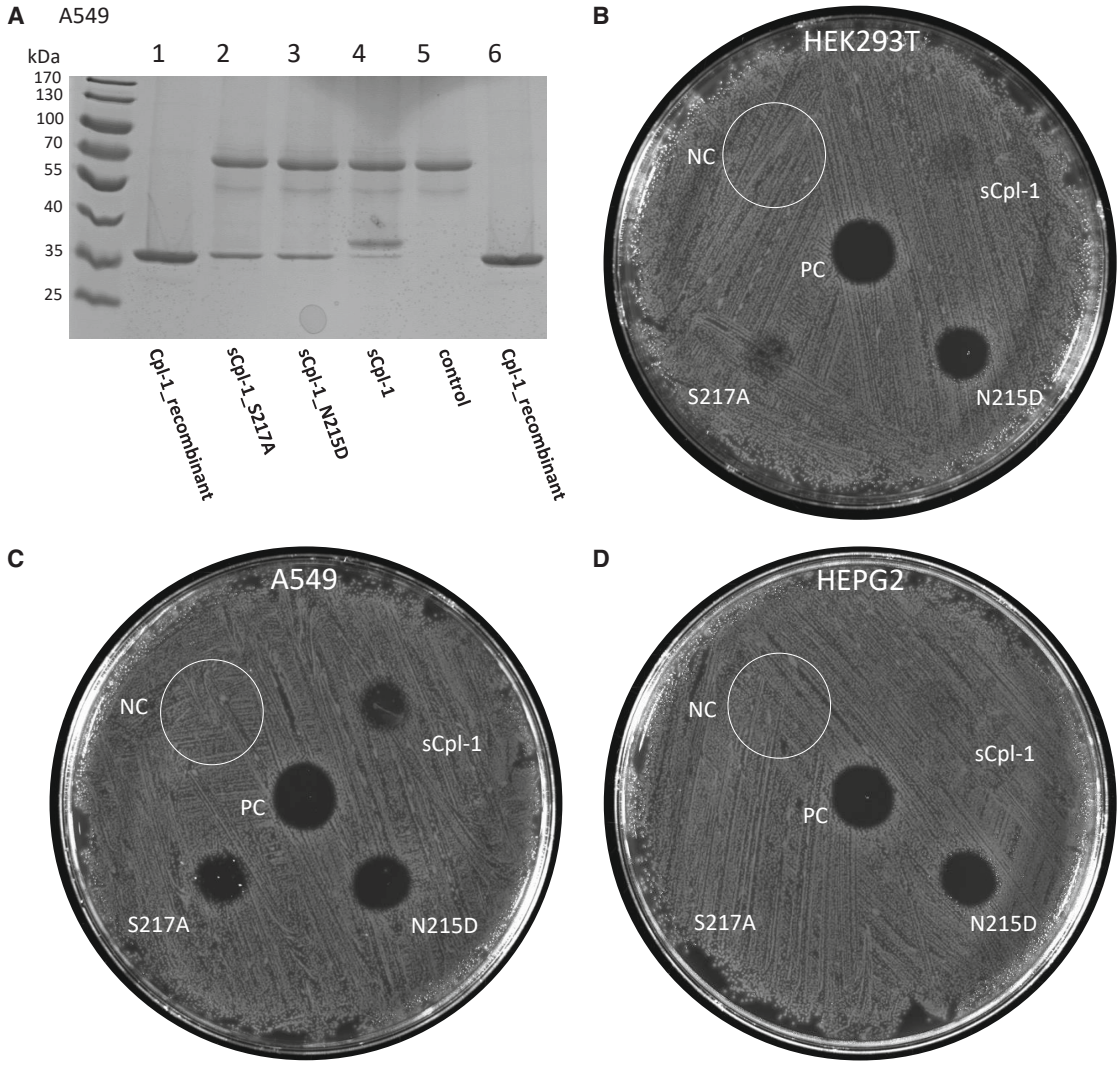


**Figure 5. Investigation of supernatant samples of cells transfected with hlySP-sCpl-1/hlySP-sCpl-1N215D/hlySP-sCpl-1S217A-encoding mRNA**

(A) Concentrated serum-free supernatants of A549 cells transfected with hlySP-sCpl-1S217A (2)/hlySP-sCpl-1N215D (3)/hlySP-sCpl-1 (4)-encoding mRNA were subjected to SDS-PAGE; recombinant Cpl-1 (1.75 μg, ca. 37 kDa) (1 and 6), control (5). (B–D) Assessement of lysis zones on blood agar plates. The plates were inoculated with pneumococcal suspension (McFarland 0.5). Ten microliters of concentrated supernatant from HEK293T (B), A549 (C), and HepG2 (D) cells harvested 24 h after transfection with hlySP-sCpl-1 (sCpl-1)/hlySP-sCpl-1N215D (N215D)/hlySP-sCpl-1S217A (S217A)-encoding mRNA was spotted on plates 16 h before readout; NC: negative controls are within area of white circle; PC: 10 μL of recombinant Cpl-1 (10 μg/mL) was spotted in center of each plate as positive control.

performed. Transfection with 250 ng of mRNA resulted in a less pronounced killing effect from concentrated supernatants compared with the higher doses in all three cell lines; however, the difference was noticeably less pronounced for A549 cells (log reductions: 1.25 for HEK293T [$p < 0.001$], 2.24 for A549 [$p < 0.01$], and 0.75 for HepG2 cells [$p < 0.001$]). The killing effect after transfection with 500 ng and 1,000 ng of mRNA appeared to be very similar in all three cell lines (difference between log CFU reductions: 0.02 for HEK293T, 0.24 for A549, and 0.02 for HepG2 cells) (Figures 7A–7C). Based on these observations, the use of 500 ng was continued in the following transfection experiments.

### Cpl-1N215D in A549 culture supernatants led to a noticeable killing effect after 6 h and increased incrementally until 24 h post-transfection

The influence of time after transfection on the expression of hlySP-sCpl-1N215D was determined by testing the pneumococcal killing effect in supernatant of A549 cells collected at the following time points: 6 h, 12 h, 24 h, 48 h, 72 h. Samples were used for turbidity reduction experiments (Figure S7D) and subsequent determination of CFU. Six hours post-transfection, a killing effect was noticeable (Figure 7D) that incrementally increased over later time points (log reductions after 6 h: 0.65 [$p = 0.01$]). However, after 24 h the increase became

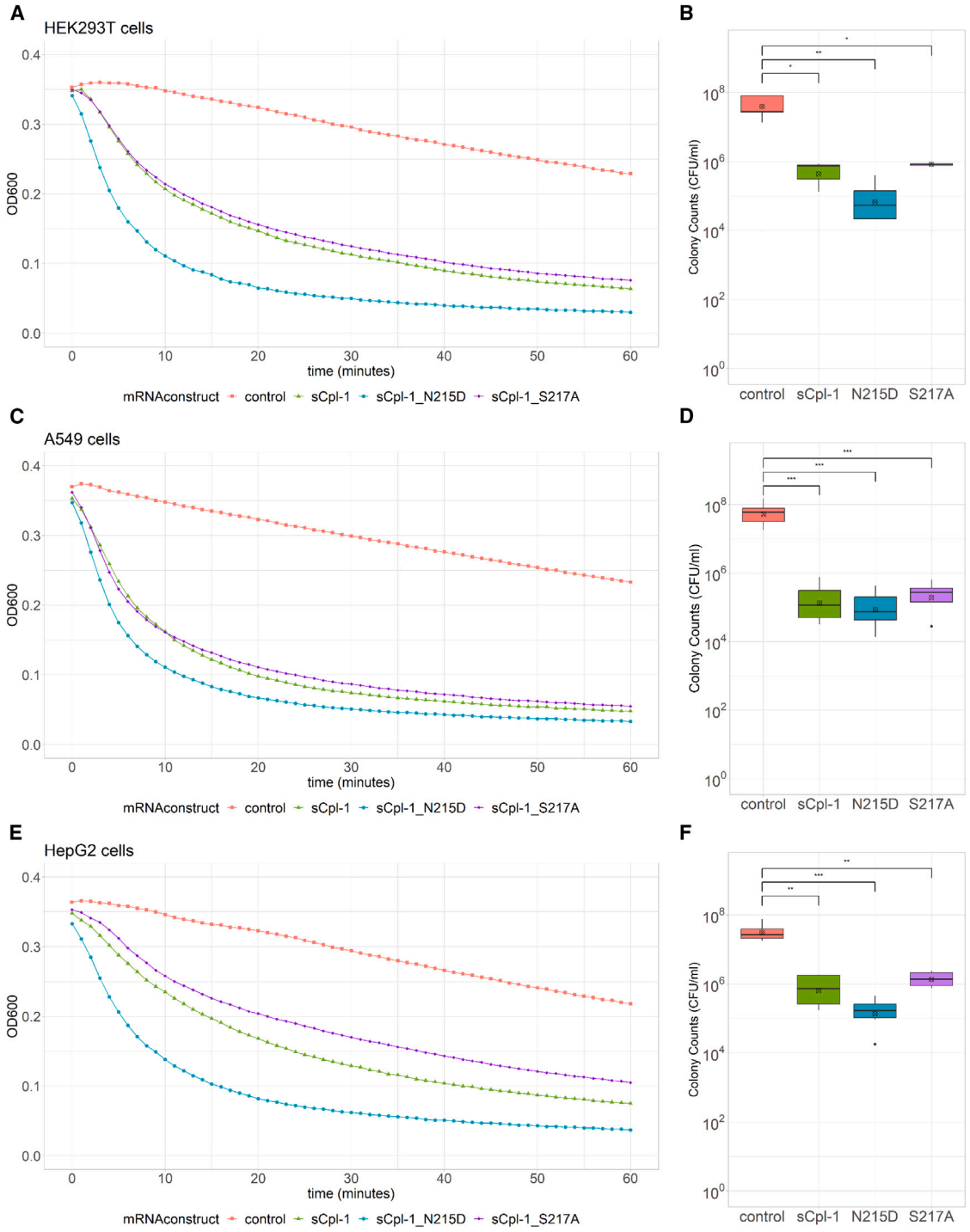


**Figure 6. Bacteriolytic effect of concentrated supernatant samples from HEK293T/A549/HepG2 cells transfected with hlySP-sCpl-1/hlySP-sCpl-1N215D/ hlySP-sCpl-1S217A encoding mRNA against *S. pneumoniae***

(A, C, E) Turbidity reduction experiments. Twenty-two microliters of concentrated supernatant or control were applied to 200 μL of pneumococcal suspension in PBS (pH 7.0). Data from representative experiments are shown. (B, D, F) After turbidity measurements, samples were plated on blood agar and colonies were counted after 16 h. Data are based on at least three independent experiments. Boxplots represent minimum, maximum, median values, and the interquartile range. The mean is represented by a crossed circle, p values <0.05 are indicated (*p <0.05–0.01, **p < 0.01–0.001, ***p < 0.001).

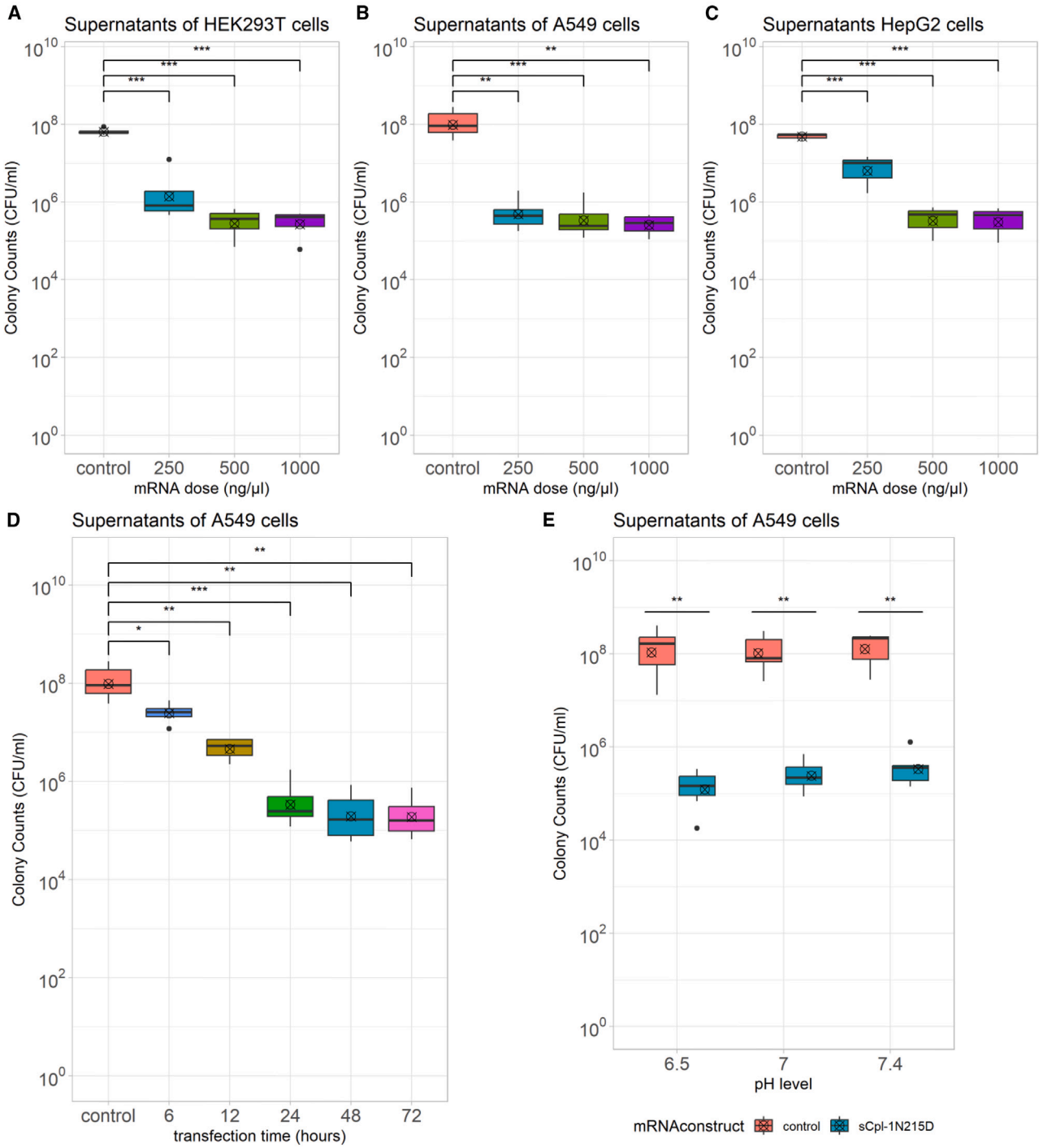


**Figure 7. Bacteriolytic effect of concentrated supernatant samples from HEK293T/A549/HepG2 cells that have been transfected with hlySP-sCpl-1N215D encoding mRNA against *S. pneumoniae***

Twenty-two microliters of concentrated supernatant or control were applied to 200 µL of pneumococcal suspension in PBS. After 60 min of incubation, samples were plated on blood agar and colonies were counted after 16 h. First row: Three different doses (250, 500, and 1,000 ng) of mRNA were administered to HEK293T cells (A), A549 cells (B), and HepG2 (C). (D) Effect of time after mRNA transfection (6, 12, 24, 48, 72 h). (E) Effect of pH on the killing effect of hlySP-sCpl-1N215D was investigated for three pH levels (6.5, 7.0, 7,4). Results are based on at least three independent experiments. Boxplots represent minimum, maximum, and median values, and the interquartile range. The mean is represented by a crossed circle, p values <0.05 were indicated (*p < 0.05–0.01, **p < 0.01–0.001, ***p < 0.001).

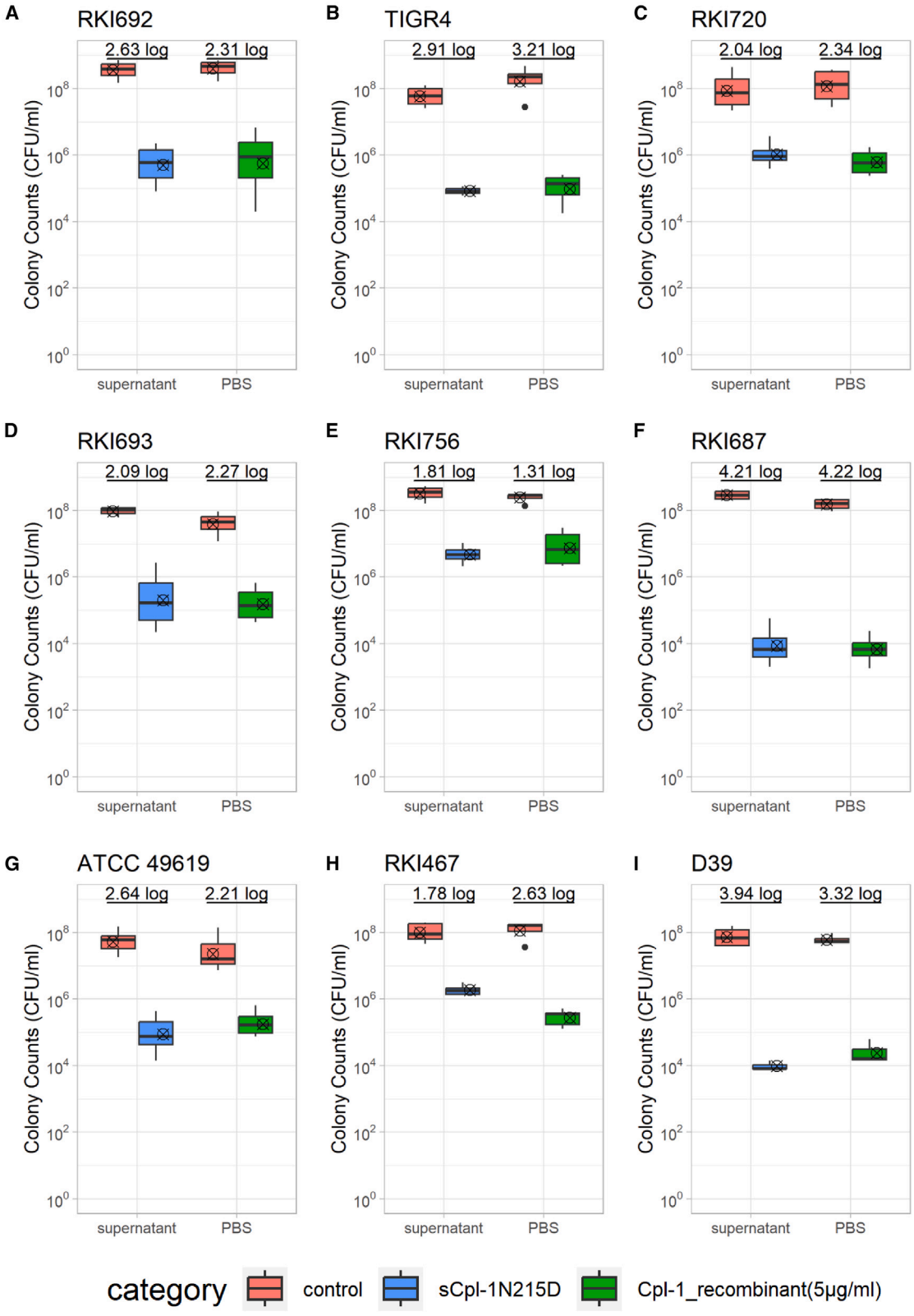


*(legend on next page)*

clearly less pronounced (difference in log CFU reduction between 24 and 72 h: 0.25). Cell viability of hlySP-sCpl-1N215D mRNA-transfected cells and controls was monitored by trypan blue uptake[45] and showed estimated cell viability of 87.3 vs. 88.0% after 24 h ($p = 0.87$, $t = 0.17$, $df = 4$), 74.7 vs. 72.3% after 48 h ($p = 0.71$, $t = 0.39$, $df = 4$), and 68.5 vs. 68.5% after 72 h ($p = 0.99$, $t < 0.01$, $df = 4$).

### hlySP-sCpl-1N215D led to a comparable pneumococcal killing effect within pH range of 6.5–7.4

To evaluate the pH sensitivity of hlySP-sCpl-1N215D expressed in A549 cells at pH 6.5, 7.0, and 7.4., turbidity reduction experiments with consecutive determination of bacterial counts were conducted as described. $OD_{600}$ reductions occurred faster over 60 min of incubation for lower pH values (Figure S7E). Bacterial counts showed log reductions of 3.01 ($p < 0.01$, $t = 3.23$, $df = 11$) at pH 6.5, 2.67 ($p < 0.01$, $t = 3.48$, $df = 16$) at pH 7.0, and 2.57 ($p < 0.01$, $t = 4.16$, $df = 10$) at pH 7.4 (Figure 7E).

### hlySP-sCpl-1N215D collected 24 h post-transfection from A549 cells was effective against nine clinically relevant pneumococcal serotypes

hlySP-sCpl-1N215D was tested against nine strains of clinically relevant capsule serotypes of *S. pneumoniae*. A549 cells were transfected with 500 ng of hlySP-sCpl-1N215D-encoding mRNA per well. Culture supernatants were collected 24 h post-transfection and prepared as described. As mentioned above, the average concentration of hlySP-sCpl-1N215D present in supernatants of A549 cells 24 h post-transfection has been estimated to be 3.6 μg/mL. Turbidity reduction experiments (Figure S8) and successive determination of CFUs were conducted for each strain as described; 5 μg/mL of recombinantly expressed Cpl-1 served as a positive control. Pneumococcal strains exposed to concentrated supernatant of A549 cells showed CFU reductions between 1.78 and 4.21 log (RKI692 [serotype 4]: 2.63, TIGR4 [serotype 4]: 2.91, RKI720 [serotype 6B]: 2.04, RKI693 [serotype 9V]: 2.09, RKI756 [serotype 14]: 1.81, RKI687 [serotype 18C]: 4.21, ATCC 49619 [serotype 19F]: 2.64, RKI467 [serotype 23F]: 1.78, D39 [serotype 2]: 3.94 log), which were comparable to the CFU reductions observed when exposed to the 5 μg/mL of recombinantly expressed Cpl-1 (Figure 8). Serotype 23F showed the highest discrepancy in CFU reductions between hlySP-sCpl-1N215D and recombinant Cpl-1 (1.78 vs. log 2.63 log reductions, based on four independent experiments).

## DISCUSSION

The Cpl-1 endolysin was detectable from lysates of all three human cell lines that had been transfected with Cpl-1-encoding mRNA and was shown to be active against pneumococci. Immunofluorescence staining of transfected cells suggested the cytosolic presence of Cpl-1. These findings support the idea that mRNA-encoded Cpl-1 might be a suitable agent for targeting *S. pneumoniae* inside human cells. Long believed to be exclusively extracellular, recent evidence suggests that splenic macrophages provide a reservoir for *S. pneumoniae*. It was concluded that the spleen, and not the lungs, is the major source of bacteremia calling for targeted treatment strategies to prevent pneumococcal sepsis.[46,47] IVT-mRNA delivery to the spleen to target antigen-presenting cells (APCs) has recently gained interest mainly for the development of cancer therapies.[16–18] Among other splenic APCs, transfection of splenic macrophages using ionizable lipid nanoparticles has been demonstrated.[16,22,23] mRNA-based Cpl-1 delivered to splenic macrophages could potentially clear intracellular *S. pneumoniae* to prevent fulminant forms of pneumococcal sepsis and represents a prime research field for mRNA-based Cpl-1. However, no proof of intracellular killing has been provided in this study and the feasibility of targeting intracellular pneumococci needs further investigation. The efficiency of intracellular Cpl-1 could be influenced by factors related to the intracellular lifestyle of the pneumococcus such as residence within vacuoles, which is assumed for cardiac myocytes.[48] Depending on pathogen- and host-specific features, the mRNA-based approach to endolysin therapy could prove useful to treat various diseases caused by intracellular pathogens such as *S. pyogenes* or mycobacterial species.[49,50]

Respiratory tract infections are the most common form of pneumococcal disease, often preceded by pneumococcal colonization.[51] Considered to be an extracellular pathogen in respiratory tract disease, secretion of mRNA-based Cpl-1 for targeting of *S. pneumoniae* seems essential for these forms of pneumococcal disease.[52] Supernatants of cells transfected with Cpl-1-encoding mRNA showed a slight lytic effect most prominent in HepG2 cells, suggestive of the presence of comparatively small amounts of Cpl-1. The reasons for the presence of the non-secretory Cpl-1 in culture supernatant have not been further investigated in this study. Possible explanations include Cpl-1 leakage through degraded cell membranes or secretion through unconventional protein secretion pathways.[53] A more prominent pneumococcal killing effect by samples from the culture supernatant could be achieved after fusion of a choice of SP-encoding nucleotides to the 5′ end of Cpl-1-encoding mRNA. Effective delivery of hlySP-sCpl-1N215D-encoding mRNA to the respiratory tract is a prerequisite to target extracellular *S. pneumoniae* for epithelial decolonization or to treat respiratory tract infections. mRNA transfection of the lungs has recently made considerable progress, for example the use of polymer-based transfection reagents such as hyperbranched poly(beta amino esters) (hPBAEs) in aerosolized form has been described to be effective for mRNA delivery in multiple animal

**Figure 8. Bacteriolytic effect of concentrated supernatant samples from A549 cells that have been transfected with hlySP-sCpl-1N215D-encoding mRNA against nine different strains of *S. pneumoniae* compared with 5 μg/mL recombinant Cpl-1**

Twenty-two microliters of samples were applied to 200 μL of pneumococcal suspension in PBS. After 60 min of incubation, samples were plated on blood agar and colonies were counted after 16 h. Results from culture supernatant are represented by blue boxes, results from recombinant Cpl-1 are represented by green boxes, respective controls are red. Results are based on at least three independent experiments, log CFU reductions are indicated for comparison. Boxplots represent minimum, maximum, and median values, and the interquartile range. The mean is represented by a crossed circle.

models.[20,21] The accumulation of mRNA-based endolysins in cell culture supernatant as shown in this study provides a base to further investigate the targeting of extracellular pathogens.

PTMs, such as N-linked glycosylation uncommon in bacteria but common in mammalian cells,[43] might lead to unwanted changes of protein properties in heterologous expression. N-linked glycosylation of the hlySP-sCpl-1 at position N215 on the endolysin's cell wall binding domain led to a reduced pneumococcal killing effect, suggesting that the glycan might have interfered with the enzyme's choline binding sites crucial for pneumococcal cell wall binding.[29] N-linked glycosylation was prevented by introduction of point mutations in the glycosylation site. However, PTMs affecting other parts of the amino acid sequence such as O-linked glycosylation, which are more difficult to predict, cannot be ruled out and need to be studied in the future. Suitability of other endolysins for the mRNA-based approach might depend on glycosylation patterns and other PTMs. While glycans attached to critical regions of the amino acid sequence can hamper with enzymatic activity on the one hand, glycans attached to other regions could confer favorable side effects. Glycosylation increases the solubility of secretory proteins and is used by viral proteins as a strategy to evade immune detection.[54] Deliberate introduction of N-linked glycosylation sites has been used to increase serum half-life of human growth hormone.[55] Introducing glycosylation sites at suitable regions of the amino acid sequence could thus be used to increase endolysin solubility and serum half-life and reduce immunogenicity. Crucially, site-directed introduction of glycosylation sites might prove superior to previous attempts to stabilize the protein. For instance, PEGylation resulted in an almost complete loss of Cpl-1 enzymatic activity.[56] This aspect highlights a possible advantage of an mRNA-based approach to endolysin therapy since amino acid changes can easily be introduced in the mRNA constructs prior to target cell transfection.

The capability of effective cell wall lysis with species or genus specificity and the lack of reported resistance counts among the most important characteristics of bacteriophage-encoded endolysins.[1,2] The latter is a significant advantage over bacteriophage therapy, which is regularly limited by resistance of the bacterial host.[57] The Cpl-1 endolysin has been found to be effective against various pneumococcal serotypes.[30] While prominent serotype-dependent differences in the killing efficiencies were observed in this study, the differences of the killing effect of recombinantly produced Cpl-1 and human cell line produced hlySP-sCpl-1N215D was within 1 log reduction for each serotype when applied at similar concentrations. This comparison suggests that the mRNA-encoded hlySP-sCpl-1N215D has retained the pneumococcal killing effect of recombinantly produced Cpl-1. However, direct comparison of the activity is limited by the fact that the concentration of the hlySP-sCpl-1N215D in the supernatant was only estimated following mass spectrometry. Furthermore, the influence of the N-terminal histidine tag of the recombinant Cpl-1 on protein activity is not known.

Results from our study suggest that endolysin-encoding mRNA applied in a sufficient dose to target cells can result in a meaningful bacteriolytic effect within a few hours. However, our study is limited to cell culture experiments not reflective of mRNA transfection of specific organs *in vivo*. In the human body, the killing effect of endolysins will be strongly influenced by the volume of distribution and other factors such as proteases or immunologic effects that are known to adversely affect concentrations and/or enzymatic activity.[1,4,5] To minimize the concentrations required to kill a pathogen, mRNA-based endolysins could target organs/tissue compartments in which the physiological environment approaches the endolysin's optimal reaction conditions. The Cpl-1 endolysin has been reported to have a pH optimum around 4–5 with enzymatic activity dropping sharply in alkaline conditions.[30] While physiological pH in blood is around 7.4, pH of airway surface liquid seems to be slightly acidic under physiological conditions with pH values ranging between 5.6 and 6.7 in the nasal mucosa and around 7.0 in the bronchia.[58] Experiments in this study have been conducted at pH 7.0 as a default, the effect of slightly lower (6.0) and higher (7.4) pH values within physiological boundaries were additionally assessed for the hlySP-sCpl-1N215D. $OD_{600}$ reductions occurred faster over 60 min of incubation at lower pH values but resulted in comparable CFU reductions. It is therefore assumed that the hlySP-sCpl-1N215D could be effective within body compartments of differing pH ranges, if its presence over a sufficient period of time can be ensured.

The human lysozyme SP was selected as the presumably most potent SP based on the differences in pneumococcal killing effect of sCpl-1 in supernatant samples. However, differences between mRNA constructs carrying the various SPs used in this study might not solely reflect the secretion efficiency. As expression levels of IVT-mRNA have been shown to be dependent on mRNA design choices, the observed differences could be a result of different expression levels of the distinct mRNA constructs.[25,26] More generally, the influence on variations of parameters such as the 5′ and 3′ UTR regions, SP, nucleotide modifications, and length of poly(A) tail on mRNA expression should be further investigated.

While the observed pneumococcal killing efficiencies of supernatant samples containing hlySP-sCpl-1N215D seemed relatively comparable between cell lines, lysate samples of HEPG2 cells containing Cpl-1 showed a less prominent effect (>1 log less than HEK293T or A549 cells). Possible reasons for these cell-specific differences comprise varying transfection efficiencies, mRNA expression levels, or cytosolic stability. Cell-specific optimization of these parameters will be crucial to enable efficient endolysin production of target cells in future studies.

Supernatant concentrations of hlySP-sCpl-1N215D did not increase significantly after 24 h in A549 cells. Decreased viability of cells in culture beyond 24 h post-transfection as indicated by trypan blue staining might have affected translation efficiencies but the role of cytosolic stability of the used mRNA constructs needs further investigation.

No meaningful difference in cell viabilities between transfected and non-transfected cells was observed in this study. Mass spectrometric

analyses that were primarily performed for the detection of Cpl-1 showed no evidence of differential expression of other proteins between transfected and non-transfected cells in all cell lines. However, this finding is limited by a low number of controls (n = 2 per cell line) and the effect of Cpl-1/hlySP-sCpl-1N215D-encoding mRNA on cells should be further investigated.

The success of future endolysin therapies depends on innovative methods to administer proteins at the sites of infection in the human body. To the best knowledge of the authors, the results of this study show for the first time that human cells are in principle capable of mRNA-based endolysin production as demonstrated using the Cpl-1 endolysin. mRNA-based expression of the cytosolic Cpl-1 endolysin and its secretory variant hlySP-sCpl-1N215D allow selection between intracellular and extracellular Cpl-1 localization. Coupled with recently described mRNA delivery vehicles, the mRNA constructs are potential candidates for the treatment of non-invasive and invasive forms of pneumococcal disease. As innovative solutions are urgently needed to tackle the global antibiotics resistance crisis, the mRNA-based approach to antibiotic therapy described in this study should be further investigated.

## MATERIALS AND METHODS

### Recombinant Cpl-1 production

The gene of the Cpl-1 endolysin of the *Streptococcus* phage Cp-1 (Genebank accession number: NC_001825.1) was codon-optimized using the Azenta codon optimization tool (Azenta, Chelmsford, USA) and appended with a C-terminal histidine tag (6xHis). Gene synthesis and cloning into a pET-21(+) expression vector was done by Twist Bioscience (South San Francisco, California). *E. coli* BL21(DE3) was transformed with the resulting plasmid pET-21(+)_Cpl-1. A clone was selected and incubated in 500 mL LB medium with ampicillin (100 mg/L) at 37°C until $OD_{600}$ reached 0.5. Expression was induced using 0.5 mM IPTG, culturing was continued on a shaker at 20°C overnight. Aliquots of 250 mL were centrifuged at 4,000 × *g* for 15 min and pellets were frozen at −20°C. Pellets were thawed, suspended in 5 mL lysis buffer (50 mM $NaH_2PO_4$, 300 mM NaCl, 10 mM imidazole, pH 8.0) before lysis on a tissue homogenizer (Precellys 24, bertin technologies) (2 cycles at 6,500 rpm for 30 s, samples were placed on ice for 5 min between cycles). Samples were then centrifuged at 13,000 × *g* for 15 min. The supernatant was transferred in a 15-mL tube with 1 mL Ni-NTA Agarose (Invitrogen, Carlsbad, CA, USA) and moved on a Stuart SB3 Rotator at 4°C for 90 min (Cole Parmer, Wertheim, Germany). The sludge was placed on a 10-mL filter column with 35-µm pore size (MoBiTec, Goettingen, Germany). Washing and elution were carried out using the respective buffers (wash buffer: 50 mM $NaH_2PO_4$, 300 mM NaCl, 20 mM imidazole, pH 8.0; elution buffer: 50 mM $NaH_2PO_4$, 300 mM NaCl, 250 mM imidazole, pH 8.0), the fractions were analyzed using SDS-PAGE (12%). Elution fractions were combined, dialyzed against PBS, and quantified using a Qubit 4 fluorometer (Invitrogen).

### mRNA preparation

The Cpl-1 nucleotide sequence was codon-optimized for the purpose of heterologous expression in human cells using the Azenta Codon Optimization tool (Azenta). DNA templates containing the 5′ UTR of the human alpha globin gene, the Cpl-1 gene, and the 3′ UTR of the human alpha globin gene were synthesized by Twist Bioscience (South San Francisco, CA) and cloned into a vector (pTwist Amp High Copy). To facilitate secretion of the Cpl-1 endolysin, constructs were modified to contain an SP-encoding nucleotide sequence at the 5′ end of the open reading frame (Table S2). Prior to IVT, vector DNA containing the templates was PCR amplified using Phusion High-Fidelity DNA-Polymerase (Thermo Fisher Scientific) according to the manufacturer's protocol. A reverse primer with a poly(T)-tail of 120 bp was attached to the 5′ end, which was translated into a poly(A)tail on the leading strand (forward primer: 5′-CAATCAC CACGAGACATTAATACGACTCAC-3′, reverse primer: 5'-(120xT) GCTGCCCACTCAGACTTTATTCAAAGAC-3′); Reaction protocol: 98°C for 30 s, 30 cycles at 98°C for 10 s, 68°C for 30 s, and 72°C for 25 s, and final extension at 72°C for 10 min dsDNA templates were purified using QIAquick PCR Purification Kit (Qiagen) and subjected to IVT reactions using the HiScribe T7 mRNA Kit with CleanCap Reagent AG (New England Biolabs, Ipswich, MA, USA), which co-transcriptionally adds a natural Cap-1 structure (meaning that the first base of the mRNA is methylated at the 2′ position) to the 5′ end. Briefly, 800 ng of PCR template was added to a 20-µL reaction volume prepared according to the manufacturer's recommendations. Uridine nucleotides were completely substituted by N1-methylpseudouridine (TriLink BioTechnologies, San Diego, CA, USA) in an equimolar fashion. IVTs were conducted at 37°C overnight. After IVT, DNA templates were cleaved using DNase I (NEB) according to the manufacturer's recommendations. The RNA product was purified using the Monarch RNA Cleanup Kit (NEB) and eluted in nuclease-free water (NEB). mRNA was quantified using Qubit dsDNA HS Assay-Kit (Thermo Fisher Scientific) and adjusted to a concentration of 100 ng/µL. mRNA was quality-checked using mRNA gel electrophoresis. Aliquots were stored at −80°C.

### Human cell lines

HEK293T cells (ACC 635) derived from the kidney of a human embryo and A549 cells (ACC 107) derived from human adenocarcinoma alveolar epithelial cells were purchased from DSMZ and grown in DMEM (high glucose, GlutaMAX supplement and pyruvate) (Thermo Fisher Scientific) supplemented with 10% fetal bovine serum (FBS). HepG2 cells (ACC 180) derived from a hepatocellular carcinoma were purchased from DSMZ and grown in Eagle's Minimum Essential Medium (CLS, Eppenheim, Germany) supplemented with 10% FBS. Cells were cultured in 75 $cm^2$ culture flasks with adherent cell culture surface (Greiner Bio-One, Frickenhausen, Germany).

### Transfection of cell lines

Transfection experiments were conducted in a 24-well plate format (Greiner Bio-One) in duplicate, i.e., cells of two wells were transfected

with the same mRNA construct, samples were combined at collection. Cells were dissociated from culture flasks using trypsin-EDTA (0.25%) (Thermo Fisher Scientific), transferred to 24-well plates, and cultured in 500 μL medium per well for 24 h to reach 70%–100% confluency prior to transfection. Varying amounts of mRNA (250/500/1,000 ng per well) were combined with Lipofectamine MessengerMAX (Thermo Fisher Scientific) (1.5 μL per well) in Opti-MEM reduced serum medium (Thermo Fisher Scientific) to form mRNA-lipid complexes according to the manufacturer's instructions. mRNA-lipid complexes contained in reduced serum medium were then added to the culture medium of cells in the plates. Controls were treated in the same way but instead of mRNA an equal volume of PBS was used. Success of mRNA transfection was ascertained by running a positive control using CleanCap EGFP mRNA (TriLink BioTechnologies).

#### Processing of transfected cells

At a defined period (6/12/24/48/72 h) post-transfection, culture supernatants were removed from well plates and processed as described in the next paragraph. Cells were harvested using 200 μL trypsin-EDTA (0.25%) (Thermo Fisher Scientific) per well, duplicates were combined in 1.5-mL tubes. Wells were then washed using 200 μL PBS. The cell suspension was centrifuged at 2,000 × *g* for 5 min at 10°C. The supernatant was discarded and cells were subjected to osmolysis using 81 μL of distilled water and three subsequent freeze-thaw cycles. Lysis was stopped by addition of 9 μL 10-fold concentrated PBS followed by centrifugation at 16,000 × *g* for 15 min (4°C). The cell lysate (∼100 μL) was transferred to 1.5-mL tubes and used for subsequent analysis.

#### Processing of cell culture supernatants

Culture supernatants of transfected cells and non-transfected controls were transferred to Amicon Ultra-4 filter tubes (Merck Millipore, MA, USA) with 30-kDa cutoff and centrifuged at 4,000 × *g* for 10 min. The concentrate was washed twice by adding an equal volume of PBS (pH 7.0) to the filter units followed by centrifugation until volume corresponded to a 10-fold concentration of the original volume, referred to in this article as "concentrated supernatants" (i.e., the combined original 1,000 μL volume from two 24-well plates resulted in 100 μL of concentrated supernatant).

#### Immunocytochemistry analysis

A549 cells were transferred to 24-well plates with plastic cover slips (Nunc Thermanox, Thermo Fisher Scientific) placed at the bottom and cultured in 500 μL medium per well for 24 h to reach 70%–100% confluency prior to transfection. mRNA transfection was conducted as described above. Twenty-four hours after transfection the medium was removed, and cells were washed with PBS and fixed using 4% paraformaldehyde. Cells were then permeabilized using 0.5% PBST for 10 min, followed by blocking using PBS with 5% FBS. Cells were incubated with a polyclonal anti-Cpl-1 antibody (Davids Biotechnologie GmbH, Regensburg, Germany) for 2–3 h. After washing thoroughly with PBS, a conjugated secondary antibody was applied for 2–3 h (Goat anti-Rabbit IgG [H + L], DyLight 594, Thermo Fisher Scientific). After washing with PBS, DAPI (300 nM, Thermo Fisher Scientific) was applied for 5 min. Coverslips were then placed on a microscope slide with mounting medium (ROTIMount FluorCare, Carl Roth GmbH, Karlsruhe, Germany). The samples were analyzed using a fluorescence microscope (Olympus BX60, Olympus, Tokyo, Japan), and pictures were taken using an RT Color CCD Camera (Diagnostic Instruments Inc, Sterling Heights, USA).

#### Pneumococcal capsule serotypes used in the study

*S. pneumoniae* strain ATCC 49619 (serotype 19F) was used as a reference strain, which was used for all experiments. Other strains tested in this study were RKI692 (serotype 4), TIGR4 (serotype 4), D39 (serotype 2), RKI720 (serotype 6B), RKI467 (serotype 23F), RKI756 (14), RKI693 (serotype 9V) and RKI687 (serotype 18C), which were kindly provided by the German reference laboratory for streptococci, Institute of Medical Microbiology Uniklinik RWTH Aachen.

#### Bacteriolytic activity against *S. pneumoniae*

##### *Assessment of pneumococcal lysis zones on blood agar plates*

For screening of bacteriolytic activity, blood agar plates were coated with a 0.9% NaCl suspension of *S. pneumoniae* (ATCC 49619) (McFarland Standard 0.5). After drying of the bacterial suspension, 10 μL of cell lysate/concentrated cell supernatant was spotted on the plates followed by overnight incubation at 37°C in a 5% $CO_2$ atmosphere. Plates were checked for the presence of lysis zones the following day.

##### *Turbidity reduction assay*

As a frequently used method to assess endolysin activity, turbidity reduction measurements were conducted with cell lysates or supernatants of transfected cells in a 96-well format using a Spectramax M2 microplate reader device (Molecular Devices, San Jose, CA, USA).[59] Twenty-two microliters of cell lysate or concentrated supernatant samples were added to 96-well plates in triplicate. *S. pneumoniae* (ATCC 49619) was grown in THY medium to logarithmic phase at an $OD_{600}$ of about 0.4 and then centrifuged at 2,300 × *g* for 10 min. The supernatant was discarded, and bacteria were washed, centrifuged again, and resuspended in PBS (pH: 7.45/7.00/6.50) to an $OD_{600}$ of 0.9 using a spectrophotometer (DeNovix, Wilmington, USA). Two hundred microliters of *S. pneumoniae* in PBS were then added to lysate or concentrated supernatants in 96-well plates (corresponding to a 10-fold dilution of previously 10-fold concentrated culture supernatant) resulting in an initial $OD_{600}$ of between 0.35 and 0.4. Pneumococcal solution was also combined with recombinantly expressed Cpl-1 endolysin (final concentration of 5 μg/mL) as a positive control. Turbidity at $OD_{600}$ was measured at 37°C once per minute for 60 min. After the experiment, samples and controls were plated on blood agar following 10-fold serial dilutions. Colonies were counted after overnight incubation at 37°C in a 5% $CO_2$ atmosphere.

#### Removal of N-linked glycans using PNGase F

To assess N-linked glycosylation of secretory Cpl-1 (sCpl-1), A549, HEK293T, and HepG2 cells were prepared for transfection as

described. Before transfection, the culture medium was replaced with serum-free medium (not supplemented with FBS). Twenty-four hours post-transfection, culture supernatant was collected, processed as described, and successively heated at 90°C for 10 min. Per PNGase F reaction, 10 μL of concentrated supernatant was used under non-denaturing conditions and 9 μL was used under denaturing conditions according to the manufacturer's recommendations. Following the reaction, samples with and without PNGase F treatment were subjected to SDS-PAGE for comparison.

#### SDS-PAGE

For SDS-PAGE analysis of supernatant samples, cell culture medium was replaced with serum-free medium prior to mRNA transfection. Cell lysates and culture supernatant samples were then prepared as described above. Cell lysates and concentrated supernatants were separated on 12% polyacrylamide gels. Gels were stained using Coomassie Brilliant blue G 250 (Merck Millipore).

#### Proteomics methods

Cell lysates and concentrated serum-free culture supernatants of three biological replicates of mRNA-transfected cells from each cell line were digested with trypsin and applied to mass spectrometry. Liquid chromatography-mass spectrometry analyses were carried out using a nanoAcquity UPLC system (Waters, Manchester, UK) coupled to a Waters Synapt G2-S mass spectrometer. Label-free protein quantification was performed using Progenesis QI for Proteomics (Nonlinear Dynamics, Newcastle upon Tyne, UK). A detailed description of the experimental procedures is provided in the supplemental material.

#### Data analysis and statistics

Data were analyzed and visualized using R (version 4.2.2). Differences between two groups were calculated using two-tailed t test, for comparison of multiple groups against one control Dunnett's test was used. Results are based on at least three independent experiments. p values <0.05 were considered significant. For t test results, t values and degrees of freedom (df) are provided in brackets.

## DATA AND CODE AVAILABILITY

Data that support the findings of this study not presented in the manuscript or supplemental material are available from the corresponding author upon reasonable request.

## SUPPLEMENTAL INFORMATION

Supplemental information can be found online at https://doi.org/10.1016/j.omtn.2024.102145.

## ACKNOWLEDGMENTS

Support for the work of M.J. and D.N. was provided by the University Medicine Rostock (FORUN 889003). We would like to thank Yvonne Humboldt and Jana Bull for technical support in the laboratory. We would like to thank Marc van der Linden (German Reference Laboratory for Streptococci, Institute of Medical Microbiology Uniklinik RWTH Aachen) for providing the pneumococcal strains used in this study. The study was performed without using human or animal subjects.

## AUTHOR CONTRIBUTIONS

M.J. had the initial idea, performed *in silico* design of mRNA constructs, conceptualized and performed experiments, managed all lab work, analyzed data, and wrote the manuscript; D.N. performed experiments; S.M. performed proteomics analysis, reviewed and revised the manuscript; C.W. and M.J. performed experiments; P.W. provided laboratory resources and critically reviewed the manuscript; B.K. provided laboratory resources, critically reviewed the study and provided helpful discussion, and critically reviewed and revised manuscript; and N.P. helped design experiments, critically reviewed the study and provided helpful discussion, and critically reviewed and revised the manuscript.

## DECLARATION OF INTERESTS

The authors declare no competing interests. The University of Rostock has filed for a patent related to this work (Application No. PVA11332DE).

## REFERENCES

1. Murray, E., Draper, L.A., Ross, R.P., and Hill, C. (2021). The Advantages and Challenges of Using Endolysins in a Clinical Setting. Viruses *13*, 680.
2. Roach, D.R., and Donovan, D.M. (2015). Antimicrobial bacteriophage-derived proteins and therapeutic applications. Bacteriophage *5*, e1062590.
3. Schmelcher, M., and Loessner, M.J. (2021). Bacteriophage endolysins - extending their application to tissues and the bloodstream. Curr. Opin. Biotechnol. *68*, 51–59.
4. Seijsing, J., Sobieraj, A.M., Keller, N., Shen, Y., Zinkernagel, A.S., Loessner, M.J., and Schmelcher, M. (2018). Improved Biodistribution and Extended Serum Half-Life of a Bacteriophage Endolysin by Albumin Binding Domain Fusion. Front. Microbiol. *9*, 2927.
5. Entenza, J.M., Loeffler, J.M., Grandgirard, D., Fischetti, V.A., and Moreillon, P. (2005). Therapeutic effects of bacteriophage Cpl-1 lysin against Streptococcus pneumoniae endocarditis in rats. Antimicrob. Agents Chemother. *49*, 4789–4792.
6. Weng, Y., Li, C., Yang, T., Hu, B., Zhang, M., Guo, S., Xiao, H., Liang, X.-J., and Huang, Y. (2020). The challenge and prospect of mRNA therapeutics landscape. Biotechnol. Adv. *40*, 107534.
7. Lindsay, K.E., Vanover, D., Thoresen, M., King, H., Xiao, P., Badial, P., Araínga, M., Park, S.B., Tiwari, P.M., Peck, H.E., et al. (2020). Aerosol Delivery of Synthetic mRNA to Vaginal Mucosa Leads to Durable Expression of Broadly Neutralizing Antibodies against HIV. Mol. Ther. *28*, 805–819.
8. Blanchard, E.L., Vanover, D., Bawage, S.S., Tiwari, P.M., Rotolo, L., Beyersdorf, J., Peck, H.E., Bruno, N.C., Hincapie, R., Michel, F., et al. (2021). Treatment of influenza and SARS-CoV-2 infections via mRNA-encoded Cas13a in rodents. Nat. Biotechnol. *39*, 717–726.
9. Vanover, D., Zurla, C., Peck, H.E., Orr-Burks, N., Joo, J.Y., Murray, J., Holladay, N., Hobbs, R.A., Jung, Y., Chaves, L.C.S., et al. (2022). Nebulized mRNA-Encoded Antibodies Protect Hamsters from SARS-CoV-2 Infection. Adv. Sci. *9*, e2202771.
10. Atari, N., Erster, O., Shteinberg, Y.H., Asraf, H., Giat, E., Mandelboim, M., and Goldstein, I. (2023). Proof-of-concept for effective antiviral activity of an in silico designed decoy synthetic mRNA against SARS-CoV-2 in the Vero E6 cell-based infection model. Front. Microbiol. *14*, 1113697.
11. Tiwari, P.M., Vanover, D., Lindsay, K.E., Bawage, S.S., Kirschman, J.L., Bhosle, S., Lifland, A.W., Zurla, C., and Santangelo, P.J. (2018). Engineered mRNA-expressed antibodies prevent respiratory syncytial virus infection. Nat. Commun. *9*, 3999.
12. Gorsuch, C.L., Nemec, P., Yu, M., Xu, S., Han, D., Smith, J., Lape, J., van Buuren, N., Ramirez, R., Muench, R.C., et al. (2022). Targeting the hepatitis B cccDNA with a

sequence-specific ARCUS nuclease to eliminate hepatitis B virus in vivo. Mol. Ther. *30*, 2909–2922.

13. Chen, B., Chen, Y., Li, J., Wang, C., Song, W., Wen, Y., Lin, J., Wu, Y., and Ying, T. (2022). A Single Dose of Anti-HBsAg Antibody-Encoding mRNA-LNPs Suppressed HBsAg Expression: a Potential Cure of Chronic Hepatitis B Virus Infection. mBio *13*, e0161222.
14. Kisich, K.O., Heifets, L., Higgins, M., and Diamond, G. (2001). Antimycobacterial agent based on mRNA encoding human beta-defensin 2 enables primary macrophages to restrict growth of Mycobacterium tuberculosis. Infect. Immun. *69*, 2692–2699.
15. Hou, X., Zhang, X., Zhao, W., Zeng, C., Deng, B., McComb, D.W., Du, S., Zhang, C., Li, W., and Dong, Y. (2020). Vitamin lipid nanoparticles enable adoptive macrophage transfer for the treatment of multidrug-resistant bacterial sepsis. Nat. Nanotechnol. *15*, 41–46.
16. Shimosakai, R., Khalil, I.A., Kimura, S., and Harashima, H. (2022). mRNA-Loaded Lipid Nanoparticles Targeting Immune Cells in the Spleen for Use as Cancer Vaccines. Pharmaceuticals *15*, 1017.
17. Ben-Akiva, E., Karlsson, J., Hemmati, S., Yu, H., Tzeng, S.Y., Pardoll, D.M., and Green, J.J. (2023). Biodegradable lipophilic polymeric mRNA nanoparticles for ligand-free targeting of splenic dendritic cells for cancer vaccination. Proc. Natl. Acad. Sci. USA *120*, e2301606120.
18. Fenton, O.S., Kauffman, K.J., Kaczmarek, J.C., McClellan, R.L., Jhunjhunwala, S., Tibbitt, M.W., Zeng, M.D., Appel, E.A., Dorkin, J.R., Mir, F.F., et al. (2017). Synthesis and Biological Evaluation of Ionizable Lipid Materials for the In Vivo Delivery of Messenger RNA to B Lymphocytes. Adv. Mater. *29*, 1606944.
19. Guevara, M.L., Persano, F., and Persano, S. (2020). Advances in Lipid Nanoparticles for mRNA-Based Cancer Immunotherapy. Front. Chem. *8*, 589959.
20. Patel, A.K., Kaczmarek, J.C., Bose, S., Kauffman, K.J., Mir, F., Heartlein, M.W., DeRosa, F., Langer, R., and Anderson, D.G. (2019). Inhaled Nanoformulated mRNA Polyplexes for Protein Production in Lung Epithelium. Adv. Mater. *31*, e1805116.
21. Rotolo, L., Vanover, D., Bruno, N.C., Peck, H.E., Zurla, C., Murray, J., Noel, R.K., O'Farrell, L., Araínga, M., Orr-Burks, N., et al. (2023). Species-agnostic polymeric formulations for inhalable messenger RNA delivery to the lung. Nat. Mater. *22*, 369–379.
22. Cheng, Q., Wei, T., Farbiak, L., Johnson, L.T., Dilliard, S.A., and Siegwart, D.J. (2020). Selective organ targeting (SORT) nanoparticles for tissue-specific mRNA delivery and CRISPR-Cas gene editing. Nat. Nanotechnol. *15*, 313–320.
23. Gomi, M., Sakurai, Y., Sato, M., Tanaka, H., Miyatake, Y., Fujiwara, K., Watanabe, M., Shuto, S., Nakai, Y., Tange, K., et al. (2023). Delivering mRNA to Secondary Lymphoid Tissues by Phosphatidylserine-Loaded Lipid Nanoparticles. Adv. Healthcare Mater. *12*, e2202528.
24. Damase, T.R., Sukhovershin, R., Boada, C., Taraballi, F., Pettigrew, R.I., and Cooke, J.P. (2021). The Limitless Future of RNA Therapeutics. Front. Bioeng. Biotechnol. *9*, 628137.
25. Tusup, M., French, L.E., De Matos, M., Gatfield, D., Kundig, T., and Pascolo, S. (2019). Design of in vitro Transcribed mRNA Vectors for Research and Therapy. Chimia *73*, 391–394.
26. Holtkamp, S., Kreiter, S., Selmi, A., Simon, P., Koslowski, M., Huber, C., Türeci, O., and Sahin, U. (2006). Modification of antigen-encoding RNA increases stability, translational efficacy, and T-cell stimulatory capacity of dendritic cells. Blood *108*, 4009–4017.
27. Orlandini von Niessen, A.G., Poleganov, M.A., Rechner, C., Plaschke, A., Kranz, L.M., Fesser, S., Diken, M., Löwer, M., Vallazza, B., Beissert, T., et al. (2019). Improving mRNA-Based Therapeutic Gene Delivery by Expression-Augmenting 3' UTRs Identified by Cellular Library Screening. Mol. Ther. *27*, 824–836.
28. García, J.L., García, E., Arrarás, A., García, P., Ronda, C., and López, R. (1987). Cloning, purification, and biochemical characterization of the pneumococcal bacteriophage Cp-1 lysin. J. Virol. *61*, 2573–2580.
29. Hermoso, J.A., Monterroso, B., Albert, A., Galán, B., Ahrazem, O., García, P., Martínez-Ripoll, M., García, J.L., and Menéndez, M. (2003). Structural basis for selective recognition of pneumococcal cell wall by modular endolysin from phage Cp-1. Structure *11*, 1239–1249.
30. Loeffler, J.M., Djurkovic, S., and Fischetti, V.A. (2003). Phage lytic enzyme Cpl-1 as a novel antimicrobial for pneumococcal bacteremia. Infect. Immun. *71*, 6199–6204.
31. McCullers, J.A., Karlström, A., Iverson, A.R., Loeffler, J.M., and Fischetti, V.A. (2007). Novel strategy to prevent otitis media caused by colonizing Streptococcus pneumoniae. PLoS Pathog. *3*, e28.
32. Harhala, M., Nelson, D.C., Miernikiewicz, P., Heselpoth, R.D., Brzezicka, B., Majewska, J., Linden, S.B., Shang, X., Szymczak, A., Lecion, D., et al. (2018). Safety Studies of Pneumococcal Endolysins Cpl-1 and Pal. Viruses *10*, 638.
33. Ikuta, K.S., Swetschinski, L.R., Robles Aguilar, G., Sharara, F., Mestrovic, T., Gray, A.P., Davis Weaver, N., Wool, E.E., Han, C., Gershberg Hayoon, A., et al. (2022). Global mortality associated with 33 bacterial pathogens in 2019: a systematic analysis for the Global Burden of Disease Study 2019. Lancet *400*, 2221–2248.
34. Sader, H.S., Mendes, R.E., Le, J., Denys, G., Flamm, R.K., and Jones, R.N. (2019). Antimicrobial Susceptibility of Streptococcus pneumoniae from North America, Europe, Latin America, and the Asia-Pacific Region: Results From 20 Years of the SENTRY Antimicrobial Surveillance Program (1997-2016). Open Forum Infect. Dis. *6*, S14–S23.
35. World Health Organization (2017). Prioritization of Pathogens to Guide Discovery, Research and Development of New Antibiotics for Drug-Resistant Bacterial Infections, Including Tuberculosis. Technical documents (World Health Organization).
36. Andries, O., Mc Cafferty, S., De Smedt, S.C., Weiss, R., Sanders, N.N., and Kitada, T. (2015). N(1)-methylpseudouridine-incorporated mRNA outperforms pseudouridine-incorporated mRNA by providing enhanced protein expression and reduced immunogenicity in mammalian cell lines and mice. J. Contr. Release *217*, 337–344.
37. Teufel, F., Almagro Armenteros, J.J., Johansen, A.R., Gíslason, M.H., Pihl, S.I., Tsirigos, K.D., Winther, O., Brunak, S., von Heijne, G., and Nielsen, H. (2022). SignalP 6.0 predicts all five types of signal peptides using protein language models. Nat. Biotechnol. *40*, 1023–1025.
38. Güler-Gane, G., Kidd, S., Sridharan, S., Vaughan, T.J., Wilkinson, T.C.I., and Tigue, N.J. (2016). Overcoming the Refractory Expression of Secreted Recombinant Proteins in Mammalian Cells through Modification of the Signal Peptide and Adjacent Amino Acids. PLoS One *11*, e0155340.
39. Haryadi, R., Ho, S., Kok, Y.J., Pu, H.X., Zheng, L., Pereira, N.A., Li, B., Bi, X., Goh, L.-T., Yang, Y., and Song, Z. (2015). Optimization of heavy chain and light chain signal peptides for high level expression of therapeutic antibodies in CHO cells. PLoS One *10*, e0116878.
40. Attallah, C., Etcheverrigaray, M., Kratje, R., and Oggero, M. (2017). A highly efficient modified human serum albumin signal peptide to secrete proteins in cells derived from different mammalian species. Protein Expr. Purif. *132*, 27–33.
41. Kober, L., Zehe, C., and Bode, J. (2013). Optimized signal peptides for the development of high expressing CHO cell lines. Biotechnol. Bioeng. *110*, 1164–1173.
42. Barash, S., Wang, W., and Shi, Y. (2002). Human secretory signal peptide description by hidden Markov model and generation of a strong artificial signal peptide for secreted protein expression. Biochem. Biophys. Res. Commun. *294*, 835–842.
43. Khoury, G.A., Baliban, R.C., and Floudas, C.A. (2011). Proteome-wide post-translational modification statistics: frequency analysis and curation of the swiss-prot database. Sci. Rep. *1*, 90.
44. Kelleher, D.J., Kreibich, G., and Gilmore, R. (1992). Oligosaccharyltransferase activity is associated with a protein complex composed of ribophorins I and II and a 48 kd protein. Cell *69*, 55–65.
45. Crowley, L.C., Marfell, B.J., Christensen, M.E., and Waterhouse, N.J. (2016). Measuring Cell Death by Trypan Blue Uptake and Light Microscopy. Cold Spring Harb. Protoc. *2016*. pdb.prot087155.
46. Ercoli, G., Fernandes, V.E., Chung, W.Y., Wanford, J.J., Thomson, S., Bayliss, C.D., Straatman, K., Crocker, P.R., Dennison, A., Martinez-Pomares, L., et al. (2018). Intracellular replication of Streptococcus pneumoniae inside splenic macrophages serves as a reservoir for septicaemia. Nat. Microbiol. *3*, 600–610.
47. Carreno, D., Wanford, J.J., Jasiunaite, Z., Hames, R.G., Chung, W.Y., Dennison, A.R., Straatman, K., Martinez-Pomares, L., Pareek, M., Orihuela, C.J., et al. (2021). Splenic macrophages as the source of bacteraemia during pneumococcal pneumonia. EBioMedicine *72*, 103601.

48. Subramanian, K., Henriques-Normark, B., and Normark, S. (2019). Emerging concepts in the pathogenesis of the Streptococcus pneumoniae: From nasopharyngeal colonizer to intracellular pathogen. Cell Microbiol. *21*, e13077.

49. Medina, E., Rohde, M., and Chhatwal, G.S. (2003). Intracellular survival of Streptococcus pyogenes in polymorphonuclear cells results in increased bacterial virulence. Infect. Immun. *71*, 5376–5380.

50. Cohen, S.B., Gern, B.H., Delahaye, J.L., Adams, K.N., Plumlee, C.R., Winkler, J.K., Sherman, D.R., Gerner, M.Y., and Urdahl, K.B. (2018). Alveolar Macrophages Provide an Early Mycobacterium tuberculosis Niche and Initiate Dissemination. Cell host & microbe *24*, 439–446.e4.

51. Simell, B., Auranen, K., Käyhty, H., Goldblatt, D., Dagan, R., and O'Brien, K.L.; Pneumococcal Carriage Group (2012). The fundamental link between pneumococcal carriage and disease. Expert Rev. Vaccines *11*, 841–855.

52. Weiser, J.N., Ferreira, D.M., and Paton, J.C. (2018). Streptococcus pneumoniae: transmission, colonization and invasion. Nat. Rev. Microbiol. *16*, 355–367.

53. Maricchiolo, E., Panfili, E., Pompa, A., De Marchis, F., Bellucci, M., and Pallotta, M.T. (2022). Unconventional Pathways of Protein Secretion: Mammals vs. Plants. Front. Cell Dev. Biol. *10*, 895853.

54. Pandey, V.K., Sharma, R., Prajapati, G.K., Mohanta, T.K., and Mishra, A.K. (2022). N-glycosylation, a leading role in viral infection and immunity development. Mol. Biol. Rep. *49*, 8109–8120.

55. Flintegaard, T.V., Thygesen, P., Rahbek-Nielsen, H., Levery, S.B., Kristensen, C., Clausen, H., and Bolt, G. (2010). N-glycosylation increases the circulatory half-life of human growth hormone. Endocrinology *151*, 5326–5336.

56. Resch, G., Moreillon, P., and Fischetti, V.A. (2011). PEGylating a bacteriophage endolysin inhibits its bactericidal activity. Amb. Express *1*, 29.

57. Labrie, S.J., Samson, J.E., and Moineau, S. (2010). Bacteriophage resistance mechanisms. Nat. Rev. Microbiol. *8*, 317–327.

58. Zajac, M., Dreano, E., Edwards, A., Planelles, G., and Sermet-Gaudelus, I. (2021). Airway Surface Liquid pH Regulation in Airway Epithelium Current Understandings and Gaps in Knowledge. Int. J. Mol. Sci. *22*, 3384.

59. Díez-Martínez, R., de Paz, H.D., García-Fernández, E., Bustamante, N., Euler, C.W., Fischetti, V.A., Menendez, M., and García, P. (2015). A novel chimeric phage lysin with high in vitro and in vivo bactericidal activity against Streptococcus pneumoniae. J. Antimicrob. Chemother. *70*, 1763–1773.